



Research on cooperative formation flight control algorithm of dual unmanned aerial vehicles based on distributed control

Yarong Hu¹, Buyong Ren¹, Sifan Chen¹, Junyun Shen¹ and Yonglong Ma^{1,*}

¹ Linxia Power Supply Company, State Grid Corporation of China, Linxia, Gansu, 731800, China

SUMMARY: *In the carrying out of cooperative work tasks, two unmanned aerial vehicles (UAVs) can provide more advantages when compared with one single plane. This circumstance has turned into an important tendency in the development progress of UAV technology. This research uses the Newton-Euler method to establish the mathematical model of the quadrotor unmanned aerial vehicle system. After that, a fault-tolerant control arithmetic for the formation of two unmanned aerial vehicles is designed, that is based on the distributed self-triggering tactic. The self-triggering mechanism in the algorithm can acquire the information of the neighboring UAVs without continuous communication, after that, the stability of the control system is through the real-time update of the control law to be guaranteed. The effectiveness of the algorithm in cooperative formation flight control is verified by combining simulation and field flight tests. The dual UAV formation system can quickly achieve trajectory tracking stabilization, furthermore, the difference between the real moving route and the pre-designed moving track is smaller than 0.05 meters. In the progress of carrying out formation hovering operation, the track offset of the double unmanned aerial vehicle (UAV) formation system is kept within 0.03 meters. This manifestates elevated-level capability in the aspect of accuracy and reaction speed. Furthermore, the energy consumption of the algorithm which this paper puts forward on Unmanned Aerial Vehicle 1 reaches approximately 5.8×10^5 joules. This pointedly reduces the energy use of the two unmanned aerial vehicle formation. A double unmanned aerial vehicle (UAV) formation control method which depends on a distributed self-triggering way can realize the control of a double-UAV formation. This target is reached by decreased energy spending while it is effectively able to prevent collision accidents.*

KEYWORDS: *Mathematical model; distributed self-triggering; formation control algorithm; dual UAVs; cooperative formation flying*

1 Introduction

A Unmanned Aerial Vehicle (UAV) is one kind of flying machine which carries out work without having a human pilot inside its body [1]. This equipment may be controlled through remote-control systems based on radio or by its pre-arranged control mechanisms to complete special missions. When we make a comparison between piloted aircraft and UAVs, UAVs have a number of advantages. They have small volume, strong movement flexibility, have good hidden performance, put forward relatively low requirements for battlefield environment, possess stronger survival ability, hence require lower expense. At the same time, unmanned aerial machines (UAVs) are often used by people in civil aviation fields such as disaster rescue

*xmzy_fzu@163.com

<https://doi.org/10.65102/is2026616>

and help, air picture shooting, and pesticide spreading. Therefore, in the past several decades, the progress of unmanned aerial vehicles and their related technologies has been attached great importance by countries all over the world. Furthermore, these technologies have obtained a growing quantity of wide attention and are being used more broadly [2, 3]. Nevertheless, single unmanned aerial flying machines (UAVs) still continuously meet with problems such as low efficiency and a small successful rate when they carry out large-scale and complicated tasks. On the other hand, the cooperative building of many unmanned aerial vehicles can solve the contradictions on the time, space and mission-related aspects [4]. Under the situations that the task is complex and the flight area is large, the whole task can be divided into a number of simple sub-tasks. Every unmanned aerial vehicle (UAV) is installed with different checking equipment, arms, and other tools to finish its own separate tasks. Through carrying out such action, the whole task can be finished in one single try, therefore it greatly promotes the task's work efficiency.

The formation flight of unmanned aerial vehicles (UAVs) requires that every single UAV has a high degree of independent decision-making capacity and strong cooperative flight skill. Concretely speaking, the independent decision-making capability requires that unmanned aerial vehicles have the ability to perceive the environment around them, quickly process related data, make decisions, and then guide the unmanned aerial vehicles to execute control commands [6]. The property of cooperation requires that the members of the formation have the ability to form an integrated and interworking unit, hence hence hence work together in a consistent manner when facing complex flight situations [7]. Furthermore, bad weather conditions, unexpected obstacles, and delays or breakdowns in the communication network can cause the environment to become more complicated. When we implement practical tasks, unmanned aerial vehicles (UAVs), together with other environmental elements, constitute a complicated system, in which every constituent affects and constraints the other elements. Because of this, the multi-unmanned aerial vehicle system (multi-UAVS) must have the ability of fast analysis and decision-making [8]. Therefore, the cooperative constructing of multiple unmanned aerial vehicles (UAVs) possesses the advantages of high working efficiency and a high success percentage when one deals with large-scale and complicated tasks. This possesses an extremely extensive prospect in many different fields including the military, agriculture, and business. Therefore, it has obtained very much attention from the governments of all countries in the world. Nevertheless, a great number of important problems about multi-UAV cooperation formation control algorithms still need to be explored and discussed further. Domestic and oversea scholars have already done very many researches in these domains.

In the domain of Unmanned Aerial Vehicles (UAVs), which is an important technology and a notable research field, the Leader-Follower method is the most fully developed among traditional formation control technologies. Ghamry et al [9] achieved formation cooperative control between ground robot and UAV by setting Leader as a ground robot and Follower as an airborne UAV and making a formation flight controller using slip mode control. Li and his work group [10] have proposed a method for formation control which is based on the two loops of inner and outer. In the inside loop, the stable flight of a single unmanned aerial vehicle (UAV) can be realized through adjusting the angle state variables of the UAVs. At the same time, on the outside loop, the cooperative flying of many unmanned aerial vehicles is finished through utilizing the Leader-Follower strategy. Pan et al [11] designed the controller using the Leader-Follower hair law formation strategy, and for the kinematic parameters that are difficult to obtain in the controller parameters, the DSC dynamic surface control technique was proposed to solve the problem, and its closed-loop system has been eventually bounded under certain constraints, thus realizing the collision avoidance. Liu and his work companions [12] have brought forward a scattered best control method for Unmanned Aerial Vehicle (UAV) formation

groups that depends on reinforcement study. In this method, the formation system is constituted by a virtual Leader which possesses non-zero finite inputs and a quantity of Follower UAVs which have undetermined dynamics. The Leader-Follower method is a method that is direct, easy for people to understand, and not hard to be put into practice. At current stage, this method is widely utilized by people in Unmanned Aerial Vehicle (UAV) group formations. Nevertheless, on account of its excessive dependence upon the Leader, therefore if the Leader meets a situation that nobody can foresee, the whole system will be influenced.

For the shortcomings which the traditional Leader-Follower method has, researchers have done improvements in many aspects to promote the operating speed, path quality and stability of the system. We draw the inspiration from the closely connected formation flying of bird flocks that are inside the forest, Nägeli et al. [13] realized the Leader-Follower type formation cooperative flight control based on distributed control strategy by estimating the state of the formation through Kalman filter algorithm using on-board visual sensing equipment and communication equipment, and conducted the corresponding flight tests. Fareh and his working companions [14] brought forward a new method to promote the path programming and formation controlling of multi-intelligent body formation Leader-Follower systems. This method carries out the combination of neural field and newly created potential field modeling. Our purpose is to handle the hard problems which are connected with keeping the integrality of the formation, promoting the quality of the path, and ensuring real-time response ability. Cheng and his workmates [15] have expanded the Leader-Follower method which is used for the cooperative formation making of unmanned aerial vehicles (UAVs). They have made a new adaptive non-singular quick terminal sliding mode formation controller that is based on neural networks (NN-ANFTSMFC). This result was gotten through the integration of radial basis function neural networks (NNs) with an adaptive virtual parameter technique.

In addition, the method of Virtual Leader [16] is a development of the concept of Leader-Follower. Its core idea is to take the building of a multi-unmanned aerial vehicle (UAV) formation as a stiff virtual framework. Inside this frame, every unmanned aerial vehicle is regarded as a fixed spot which has a certain relative position. Therefore, when the whole formation carries on the movement, the UAVs only need to follow the motion of the corresponding fixed point which is on the rigid body. Zhang et al. [17] have brought forward a cooperative shaping method for numerous unpiloted air vehicles (UAVs) which is constructed on backstepping. In this method, the route that a virtual leader takes is acted as the direction which the formation system moves forward toward. After that, the UAVs that are left keep the formation, they follow the imaginary leader.

Another one common kind of formation control methods is the behavioral control methods. These methods are constituted by an order of single actions. Every one of these single-atom behaviors possesses its own independent objective or work task. The input sources for these behaviors can respectively be the sensation data of the unmanned aerial vehicle (UAV) or the results of the behaviors of other UAVs that are inside the system. One fundamental element in the designing of a behavior-based control system lies in the establishment of various basic behaviors. In the potential behaviors that people study, collision prevention, obstacle evasion, target exploration, formation maintenance are included, together with efficient strategies for behavior coordination. Dang and Shen [18] utilized a coordinated control method which is established on an incremental double-closed-loop PID technology. They conducted careful planning on the pre-expected flight path of the front unmanned aerial vehicle (UAV) and the expected formation among many UAVs. This doing was to guarantee the seamless and secure loading process of a multi-UAV load transportation system. Luis and his work companions [19] have proposed a new real-time planning arithmetic for the path of multi-UAV formation transformation. This algorithm builds on a strategy that is triggered by events. They also

successfully completed the procedure of exchanging indoor small-scale group structures of 10 compactly placed quadrotors. Bolandi et al [20] investigated the spacecraft formation attitude control problem in the presence of state constraints, using a virtual structure approach with a decentralized coordinated control scheme for each spacecraft for station fixing and formation holding, and the proposed global formation controller combined with local optimal controllers in order to achieve formation coordination. Fang et al [21] applied multi-intelligence body reinforcement learning to multi-UAV collaborative combat decision-making, and realized autonomous evolutionary learning for task allocation and decision-making by designing MARL algorithmic architecture, situational model, decision-making model, and reward-punishment model, and constructing a validation environment for heterogeneous UAVs collaborating in air-to-ground surprise defense and attack. Vásárhelyi et al [22] used an evolutionary optimization framework to further optimize the centralized parameters in the UAV formation research results to achieve an outdoor formation of 30 multi-rotors with a maximum speed of 20 m/s and an autonomous collision avoidance function between the aircraft. Costa and his work companions brought up a formation control method that depends on the artificial potential field for the simulation of military airplane formation flying, which realizes the autonomous formation flight and target waypoint navigation of aircraft, while reducing the computational complexity and improving the adaptability. It is obvious that the method of behavioral control possesses the property of real-time feedback, and it has a totally decentralized control framework. The core advantage of this method is that the system becomes more able to adapt and can hold the dynamic adding of unmanned aerial vehicles (UAVs). One disadvantage is that to carry out mathematical analysis and the corresponding stability analysis of this system is a very hard work. This procedure possesses greater complexity when put beside other methods.

Formation control methods based on consistency theory have sprung up some valuable research results in recent years, Seo and his colleagues [24] have conducted a study regarding formation control. They have designed a distributed formation controller which is established on the basis of consistency theory. Their study's results showed that so long as one guarantees the network topological structure is directed and strongly connected, the multi-vehicle system is still capable of achieving stable formation control even if a vehicle is lost during the formation flight. Most of the formation studies achieve tracking errors that are stable only in an asymptotic sense. For promoting the convergence velocity, scholars have designed many kinds of control methods which have the finite time convergence properties, Moreira and his work group [25] have brought forward a control system which is based on a virtual structural control model for a multi-robot arrangement. This arrangement includes a quadrotor unmanned aerial vehicle (UAV) and a land-based unmanned vehicle that works inside an automatic storage warehouse. Under this situation, the land-based unmanned moving vehicle has two core abilities. In the first place, it is able to provide additional energy for the quadrotor unmanned aerial vehicle. Secondly, this device can achieve the acquirement of data from the quadrotor unmanned aerial vehicle. Therefore, the independent ability of the land-based unmanned moving vehicle has been increased. Dai et al [26] investigated the predetermined performance formation assembly and retention of UAVs based on the line-of-sight (LOS) method and designed a perturbation observer using neural network approximation technique, which ensured the system stability by utilizing the dynamic surface control technique and Lyapunov's stability theorem to enable any consecutive UAVs in the formation to perform collision-free formation assembly. Wang and Xu [27] created a global-local hybrid path planning scheme for the UAV formation obstacle avoidance problem under unforeseeable situations, which established a local hierarchy through fuzzy decision-making and refined dynamic windows, gave linear and angular velocity control inputs for wide-range and close-range obstacle avoidance, respectively, and embedded constraint dynamics into local path planning. In addition, Zhou et al [28] investigated the key

technology of UAV path planning based on deep reinforcement learning, which can generate collision-free trajectories during formation assembly, and also designed a UAV formation keeping algorithm, which is able to stably maintain the formation formation shape or change the shape when necessary. Chung et al [29] performed a distributed formation flight of 50 fixed-wing UAVs in fixed-wing formation, accomplishing the full process of formation assembly for takeoff, formation flight tracking, and formation landing and touchdown, as well as a cluster control of 20 fixed-wings using a lead-wingman strategy. Brandao et al [30] proposed a multilayer control scheme that implements three UAV formation in a ballistic tracking mission, in this arrangement, a separate layer takes charge of every single aspect of the formation control problem. Each layer acts as a self-governing unit which solves a specific part of the navigation problem.

In the present research paper, a mathematics model of the unmanned aerial vehicle (UAV) system is built by us, thus, to let the in-air flight of UAVs become visible. After that, a fault-tolerant control arithmetic is put forward by us. This arithmetic method, which is built upon a distributed self-triggering strategy, is devised for one pair of UAVs that carry out flight in a cooperative formation. The algorithm contains two core parts, in which the fault-tolerant control part can determine the global formation error dynamic equation and estimate the state error based on the UAV network connectivity state. On the opposite side, the self-start tactic makes possible the gathering of unmanned aerial vehicle (UAV) condition information, therefore promoting the safety and stability of formation flying. The proposed algorithm has passed simulation and verification to prove its practical usefulness in aspects including trajectory tracking, obstacle avoidance, and energy efficiency.

2 Method

2.1 Mathematical modeling of UAS

For the development of a formation control algorithm which is used by a set of unmanned aerial vehicles (UAVs), the establishment of a model that describes the UAV's dynamic behavior is necessary. This research will use the Newton-Euler method to build a dynamic model which describes the posture and position of the quadrotor unmanned aerial vehicle.

2.1.1 Model assumptions

A quadrotor unmanned aerial vehicle (UAV) is one kind of non-linear, multi-variable, strongly coupled, under-actuated system. When we handle this kind of non-linear system, to build the dynamic model of the system is very complicated. For making the model become simpler, some hypotheses must be put forward for the quadrotor unmanned aerial vehicle:

(1) The four-rotor unmanned flying apparatus is a rigid body that possesses a very symmetrical shape and structure, together with an equally distributed body weight.

(2) The mass center and the gravity center of the four-rotor unmanned aerial vehicle superpose, and it possesses an inertia product $I_{xy} = I_{yz} = I_{zx} = 0$.

(3) The quality and inertia moment of the four-rotor unmanned aerial vehicle all keep unchanged in the time process.

(4) The rising strength which is generated by the propellers is directly proportional to the quadratic of the rotational speed of the propeller. In the same way, the opposite torque which is produced by the rotation of propellers is also directly proportional to the quadratic of the rotational velocity of the propeller.

(5) A quadrotor propeller produces the same pressure when rotating forward and reverse at the same voltage.

(6) The earth is treated as a horizontal plane, its curvature is ignored, and the ground coordinate system is considered to be an inertial coordinate system.

(7) The quadrotor UAV attitude angle is limited to the following according to the actual situation: roll angle $\phi\left(-\frac{\pi}{2} < \phi < \frac{\pi}{2}\right)$, pitch angle $\theta\left(-\frac{\pi}{2} < \theta < \frac{\pi}{2}\right)$ and yaw angle $\psi(-\pi \leq \psi < \pi)$.

(8) Odd numbered propellers rotate clockwise, even numbered propellers rotate counterclockwise, and the pull of the propeller is always perpendicular to the plane of the fuselage.

2.1.2 Coordinate system

To establish a mathematical model of a system, a coordinate system must first be established. For a quadrotor UAV, to describe clearly the motion of the UAV, it is generally necessary to establish a ground coordinate system and an airframe coordinate system.

(a) Ground coordinate system

Let the ground coordinate system be $E(o_e x_e y_e z_e)$, then the coordinate origin o_e is any chosen point on the ground. The $o_e x_e$ -axis points in any direction, the $o_e z_e$ -axis is perpendicular to the ground pointing in the opposite direction to the center of the earth, and the $x_e o_e y_e$ is a horizontal plane, which conforms to the right-handed helix rule.

(b) airframe coordinate system

Let the body coordinate system be $B(o_b x_b y_b z_b)$, then the origin o_b is at the center of mass of the UAV. The $o_b x_b$ axis is chosen to coincide with one of the brackets of the vertical cross of the quadcopter UAV, and the $o_b z_b$ axis is perpendicular to the $x_b o_b y_b$ plane pointing upwards of the UAV, which is in accordance with the law of the right-hand spiral.

(c) Euler angle

According to Euler's theorem, the rotation of a rigid body around a point can be described using three fundamental rotations in three directions. In these three basic rotations, each rotation axis corresponds to one specific coordinate axis of the coordinate system which needs rotation, and every rotation angle therefore is the Euler angle. The attitude angle of the unmanned aerial vehicle (UAV) is determined through the correlation that exists between the airframe coordinate system and the ground coordinate system. The pitch, roll and yaw angles are specifically defined as follows: the pitch angle θ is the angle between the $o_b x_b$ axis and the $x_e o_e y_e$ plane. The yaw angle ψ is the angle between the projection of the $o_b x_b$ axis on the $x_e o_e y_e$ plane and the $o_e x_e$ axis. The roll angle ϕ is the angle between the $o_b z_b$ axis and the vertical plane containing the $o_b x_b$ axis.

For the transformation from the ground coordinate system to the airframe coordinate system, three rotations must be carried out by people. These rotary motions can be obtained through first rotating around the z -axis then rotating around the y -axis and finally rotating around the x -axis, and the matrices corresponding to each of the rotations are respectively:

$$R(z, \psi) = \begin{bmatrix} \cos \psi & \sin \psi & 0 \\ -\sin \psi & \cos \psi & 0 \\ 0 & 0 & 1 \end{bmatrix} \quad (1)$$

$$R(y, \theta) = \begin{bmatrix} \cos \theta & 0 & -\sin \theta \\ 0 & 1 & 0 \\ \sin \theta & 0 & \cos \theta \end{bmatrix} \quad (2)$$

$$R(x, \phi) = \begin{bmatrix} 1 & 0 & 0 \\ 0 & \cos \phi & \sin \phi \\ 0 & -\sin \phi & \cos \phi \end{bmatrix} \quad (3)$$

After that, the rotation matrix of the coordinate system can be obtained through the multiplication of the three basic rotation matrices which were talked above.

$$R = R(z, \psi)^{-1} R(y, \theta)^{-1} R(x, \phi)^{-1}$$

$$= \begin{bmatrix} \cos \theta \cos \psi & \cos \psi \sin \theta \sin \phi & \cos \psi \sin \theta \cos \phi \\ -\sin \psi \cos \phi & +\sin \psi \sin \phi & \\ \cos \theta \sin \psi & \sin \psi \sin \theta \sin \phi & \sin \psi \sin \theta \cos \phi \\ +\cos \psi \cos \phi & -\cos \psi \sin \phi & \\ -\sin \theta & \sin \phi \cos \theta & \cos \phi \cos \theta \end{bmatrix} \quad (4)$$

2.1.3 Kinetic modeling

Dynamical models are the basis for the control of an object and describe the relationship between the forces on the object and its motion. Let $P = [x, y, z]^T \in \mathbb{R}^3$ and $V = [\dot{x}, \dot{y}, \dot{z}]^T \in \mathbb{R}^3$ be the position and velocity vectors in the terrestrial coordinate system respectively. $\chi = [\phi, \theta, \psi]^T \in \mathbb{R}^3$, and ϕ, θ, ψ denote the three attitude angles of the quadcopter UAV: roll, pitch, and yaw, respectively. $V_b = [\dot{x}_b, \dot{y}_b, \dot{z}_b]^T \in \mathbb{R}^3$ and $\omega = [\dot{\phi}, \dot{\theta}, \dot{\psi}]^T \in \mathbb{R}^3$ are the velocity vector and angular velocity vector in the body coordinate system, respectively.

The P and V are related as follows:

$$\dot{P} = V \quad (5)$$

V and V_b are related as follows:

$$V = R V_b \quad (6)$$

Define the control input as:

$$\left\{ \begin{array}{l} u_1 = \frac{b\omega_1^2 + b\omega_2^2 + b\omega_3^2 + b\omega_4^2}{m} \\ u_2 = \frac{l^*b\omega_4^2 - l^*b\omega_2^2}{I_1} \\ u_3 = \frac{l'b\omega_2^2 - l'b\omega_1^2}{I_2} \\ u_4 = \frac{C\omega_1^2 - C\omega_2^2 + C\omega_3^2 - C\omega_4^2}{I_3} \end{array} \right. \quad (7)$$

The four propeller rotational speeds do not deviate much, and it can generally be assumed that $\Omega \approx 0$, i.e., If we put aside the influence that the four propellers bring to the gyroscopic moments which are produced by the vehicle, therefore, the kinetic model equation is like this:

$$\left\{ \begin{array}{l} \ddot{x} = \frac{-K_1\dot{x}}{m} + (\sin\theta \cos\phi \cos\psi + \sin\phi \sin\psi)u_1 \\ \ddot{y} = \frac{-K_2\dot{y}}{m} + (\sin\theta \cos\phi \sin\psi - \sin\phi \cos\psi)u_1 \\ \ddot{z} = \frac{-K_3\dot{z}}{m} - g + (\cos\theta \cos\phi)u_1 \\ \ddot{\phi} = u_2 - \frac{l'K_4\dot{\phi}}{I_1} + \frac{I_2 - I_3}{I_1}\dot{\theta}\dot{\psi} \\ \ddot{\theta} = u_3 - \frac{l'K_5\dot{\theta}}{I_2} + \frac{I_3 - I_1}{I_2}\dot{\phi}\dot{\psi} \\ \ddot{\psi} = u_4 - \frac{K_6\dot{\psi}}{I_3} + \frac{I_1 - I_2}{I_3}\dot{\phi}\dot{\theta} \end{array} \right. \quad (8)$$

2.2 Formation fault-tolerant control algorithm based on distributed self-triggering strategy

2.2.1 Control objectives

For the promotion of the safety performance of the dual-unmanned aerial vehicle (UAV) formation controlling system, and for the reduction of the consumption of communication resources among the aerial vehicles, a formation fault-tolerant control algorithm based on a distributed self-triggering strategy will be proposed in this section, with the following specific control objectives and research steps:

The distributed event-triggered formation fault-tolerant control arithmetic for multiple unmanned aerial vehicles (UAVs) which depends on the state observer carries out the update of control law only in the case when the system satisfies the event-triggered condition. At the same time, the stability of the closed-loop formation control system is able to be ensured, on the condition that some attack intensity and attack frequency requirements are satisfied.

In order to avoid that the determination of the event triggering condition needs to contact to obtain the information of neighboring UAVs, the event triggering condition is improved, and a self-triggering mechanism without continuous communication is proposed. Formation Control

Objective:

$$\lim_{t \rightarrow \infty} \|X_i - X_0 - q_i\| = \lim_{t \rightarrow \infty} \|\delta_i\| = \Delta \quad (9)$$

where $\delta_i = X_i - X_0 - q_i$ denotes the formation error, and $q_i \in \mathbb{R}^{6 \times 1}$ is the UAV and the desired state offset between the long aircraft, specifically, $q_i = [q_{i,x}, q_{i,y}, q_{i,h}, q_{1 \times 3}]^T$, and Δ denotes the neighborhood near the origin.

The structure of the distributed self-triggered formation fault-tolerant control strategy is shown in Fig. 1. In order to accomplish the above control objectives, the following assumptions and lemmas are given for the analysis and design of the fault-tolerant control strategy.

Assumption 1: When $t \in \bar{\Pi}_s(t_0, t_2)$, i.e., when the communication network works normally, the communication network topology is connected.

Lemma 1: When Assumption 1 holds, the communication network matrix \mathcal{M} has only one eigenvalue constant at 0, and the remaining $N-1$ eigenroots of the matrix have positive real parts satisfying $0 = \lambda_1 < \lambda_2 \leq \dots \leq \lambda_N$.

Lemma 2: If the system is controllable and observable, the following algebraic Riccati equation has a unique symmetric positive definite matrix feasible solution $P \in \mathbb{R}^{6 \times 6}$:

$$PA + A^T P - PBB^T P + C^T C = 0 \quad (10)$$

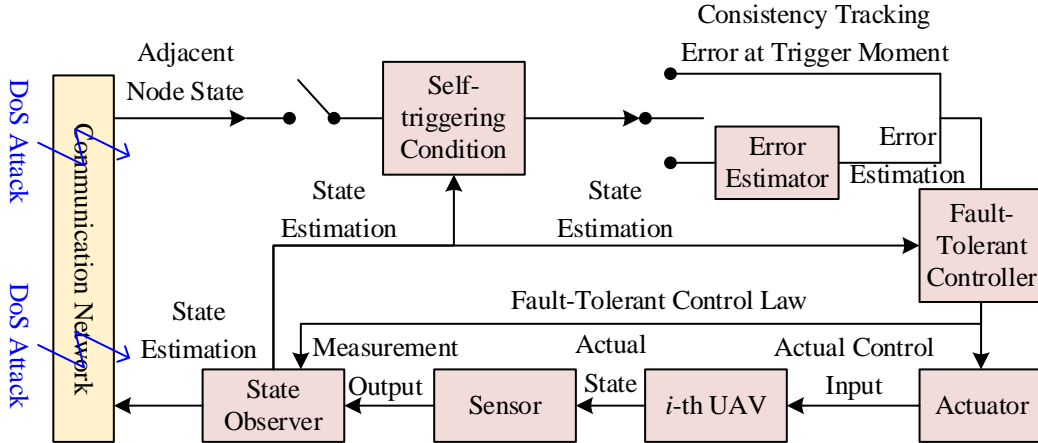


Figure 1: Distributed self-triggered formation fault-tolerant control strategy structure

2.2.2 Fault-tolerant control algorithms

Based on the network connectivity state of a dual UAV formation system, design a formation distributed fault-tolerant control law with the following form:

$$U_i = (1 - \tau)U_{hi} + \tau U_{ai} \quad (11)$$

where $U_{hi} \in \mathbb{R}^{3 \times 1}$ and $U_{ai} \in \mathbb{R}^{3 \times 1}$ are the formation control laws when the system is not attacked and when it is attacked, respectively.

The design of U_i is divided into two cases based on the value of τ in Eq.

(1) When $\tau = 0$, $U_i = U_{hi}$.

In order to obtain the velocity state of each UAV, the following decentralized state observer is designed:

$$\begin{cases} \dot{X}_i(t) = AX_i(t) + BU_{hi}(t) + H(Y_i(t) - Y_i(t)) \\ Y_i(t) = CX_i(t) \end{cases} \quad (12)$$

where $X_i(t) \in \mathbb{R}^{6 \times 1}$ and $Y_i(t) \in \mathbb{R}^{3 \times 1}$ are the state and output estimates of the i th UAV, respectively, and $H \in \mathbb{R}^{6 \times 3}$ is the state observer gain matrix.

To design the time-triggered formation control law, a series of error vectors are defined as follows:

(a) Define the coherent tracking error of the i th UAV as:

$$z_i(t) = \sum_{j=1}^N a_{ij} (X_j(t) - q_i - X_i(t) + q_j) + c_i (X_i(t) - X_0(t) - q_i) \quad (13)$$

(b) Define the measurement error of the i th UAV as:

$$\tilde{z}_i(t) = z_i(t_k^i) - z_i(t) \quad (14)$$

where t_k^i is the moment of the k th control trigger.

(c) Define the state estimation error and output estimation error of the i th UAV as:

$$\begin{cases} X_i(t) = X_i(t) - X_i(t) \\ Y_i(t) = Y_i(t) - Y_i(t) \end{cases} \quad (15)$$

According to the above equation, the dynamic equation of state estimation error can be obtained as:

$$\dot{X}(t) = (I_N \otimes (A - HC)) X(t) \quad (16)$$

where $X(t) = [X_1^T(t), X_2^T(t), \dots, X_N^T(t)]^T$.

From Eq. It is clear that the formation error signal does not have any influence on the state estimation error. As the consequence, the state estimation error can approach zero when the matrix H such that $A - HC$ is the Hurwitz matrix, i.e:

$$\lim_{t \rightarrow \infty} X_i(t) = 0 \quad (17)$$

Then, the following event-triggered control law is designed for the i th UAV:

$$U_{hi}(t) = \eta_1 K_1 z_i(t_k^i) \quad (18)$$

where $\eta_1 > 0$ is the gain coefficient, $K_1 \in \mathbb{R}^{3 \times 6}$ is the feedback gain matrix, and the triggering moment t_k^i is defined as:

$$t_{k+1}^i = \inf \left\{ t > t_k^i \mid h_1(z_i(t), \tilde{z}_i(t)) = 0 \text{ Or } h_2(z_i(t), \tilde{Y}_i(t)) = 0 \right\} \quad (19)$$

The event trigger conditions $h_1 \in \mathbb{R}$ and $h_2 \in \mathbb{R}$ are designed in the following form:

$$\begin{cases} h_1(z_i(t), \tilde{z}_i(t)) = \|\tilde{z}_i(t)\| - \sqrt{\frac{-l_1 L_1}{L_2}} \|z_i(t)\| = \|\tilde{z}_i(t)\| - \xi_1 \|z_i(t)\| \\ h_2(z_i(t), \tilde{Y}_i(t)) = \|\tilde{Y}_i(t)\| - \sqrt{\frac{-l_2 L_1}{L_3}} \|z_i(t)\| = \|\tilde{Y}_i(t)\| - \xi_2 \|z_i(t)\| \end{cases} \quad (20)$$

$\xi_1 = \sqrt{-l_1 L_1 / L_2}$, $\xi_2 = \sqrt{-l_2 L_1 / L_3}$, $L_1 = -\eta_1 + \kappa \|PHC\| + \eta_1 \kappa \|\bar{B}\| / 2 < 0$, $L_2 = \eta_1 \|B\| / 2\kappa$, $L_3 - L_4 = \|C^T\| (\lambda_N \|C\| + \|PHC\| / \kappa)$, $L_3 > L_4 > 0$, $l_1 + l_2 + l_3 = 1$, and satisfy $l_3 > 0$, $-\alpha^2 L_2 / L_1 < l_1 < -(1-\alpha)^2 L_2 / L_1$, $-\beta^2 L_3 / L_1 < l_2 < -(1-\beta)^2 L_3 / L_1$, $\alpha, \beta \in (0, 0.5)$.

From the state observer equation, δ_i satisfies $\lim_{t \rightarrow \infty} \delta_i = \lim_{t \rightarrow \infty} X_i - X_0 - q_i = \lim_{t \rightarrow \infty} X_i - X_0 - q_i$. Therefore, the global formation error dynamic equation can be obtained as:

$$\begin{aligned} \dot{\delta}(t) &= (I_N \otimes A - \mathcal{M} \otimes \eta_1 B K_1) \delta(t) \\ &\quad + (I_N \otimes H C) X(t) + (I_N \otimes \eta_1 B K_1) \tilde{z}(t) \end{aligned} \quad (21)$$

where $\delta(t) = [\delta_1^T(t), \delta_2^T(t), \dots, \delta_N^T(t)]^T$, $X(t) = [X_1^T(t), X_2^T(t), \dots, X_N^T(t)]^T$, $\tilde{z}(t) = [\tilde{z}_1^T(t), \tilde{z}_2^T(t), \dots, \tilde{z}_N^T(t)]^T$.

(2) When $\tau = 1$, $U_i = U_{ai}$.

When the system is attacked, the coherent tracking error signal $z_i(t)$ will be missing. Therefore, to reconstruct the missing signal, the following error estimator is designed:

$$\begin{cases} \dot{\hat{z}}_i(t) = A \hat{z}_i(t), & \text{Which } t \in (t_n, t_n + \bar{o}_n) \\ \hat{z}_i(t) = z_i(t), & \text{Which } t = t_n \end{cases} \quad (22)$$

where $\hat{z}_i(t) \in \mathbb{R}^{6 \times 1}$ is the estimated value and t_n is the last moment before the system is attacked. Due to the energy resource limitation of the malicious network attacker, it is assumed that $\dot{\hat{z}}_i^T(t) \hat{z}_i(t) \leq \mu$, and $\mu > 0$ is the number of normals.

Based on the above error estimator, the following control law is designed:

$$U_{ai} = \eta_2 K_2 \hat{z}_i(t) \quad (23)$$

where $\eta_2 > 0$ is the gain coefficient and $K_2 \in \mathbb{R}^{3 \times 6}$ is the feedback gain matrix.

According to the above equation, the global formation error dynamic equation can be written as:

$$\dot{\delta}(t) = (I_N \otimes A)\delta(t) + (I_N \otimes \eta_2 BK_2)\hat{z}(t) \quad (24)$$

where $\hat{z}(t) = [\hat{z}_1^T(t), \hat{z}_2^T(t), \dots, \hat{z}_N^T(t)]^T$.

2.2.3 Self-triggering conditions

The self-triggering function is designed to utilize only the state information of t_k^i at the triggering moment. Specifically, the following self-triggering function is defined:

$$\frac{\Theta}{\|A\|} \left(e^{\|A\|(t-t_k^i)} - 1 \right) - \frac{\xi_1}{1+\xi_1} \|z_i(t_k^i)\| = 0 \quad (25)$$

$$\int_{t_k^i}^t \|A - HC\| \|z_i(t_k^i)\| dt - \frac{\xi_2}{1+\xi_2} \|z_i(t_k^i)\| = 0 \quad (26)$$

Among them:

$$\begin{aligned} \Theta = & \|A\| \|z_i(t_k^i)\| + \sum_{j=1}^N a_{ij} \left(\|\eta_1 BB^T P\| \|z_j(t_k^i) - z_i(t_k^i)\| + \|H\| \|\tilde{Y}_j(t_k^i) - \tilde{Y}_i(t_k^i)\| \right) \\ & + c_i \left(\|\eta_1 BB^T P\| \|z_i(t_k^i)\| + \|H\| \|\tilde{Y}_i(t_k^i)\| \right) \end{aligned} \quad (27)$$

and $\|z_j(t_k^i)\|$ is satisfied:

$$\|z_j(t_k^i)\| = \begin{cases} \|z_j(t_k^i)\|, & \text{If } \|z_j(t_k^i)\| < t \|z_i(t_k^i)\| \\ t \|z_i(t_k^i)\|, & \text{If } \|z_j(t_k^i)\| \geq t \|z_i(t_k^i)\| \end{cases} \quad (28)$$

where $t > 0$.

Define the self-triggering function: any one of the moments that holds as the event-triggering moment.

2.3 Algorithm effectiveness test design

This section describes the deployment and effectiveness validation of the formation fault-tolerant control algorithm with distributed self-triggering strategy, which is parameterized using ROS+Gazebo to obtain the better parameters and apply them to the field flight test before performing the on-board demonstration of the control algorithm.

2.3.1 Software Simulation

The target of software simulation check is to evaluate the feasibility of the control arithmetic for fault bearing in the formation of a distributed self-triggering scheme, to ensure flight safety and reduce the risk of blowing up the airplane. The second objective is to obtain the fitting values of the parameters and coefficients in the distributed self-triggered formation fault-

tolerant control algorithm, which will greatly increase the cost and risk of the test if the physical platform is used to obtain the parameters of the algorithm.

For reproducing the real physical environment to the maximum possible degree and reducing the difference between the simulation experiment and the on-spot flight experiment, the Gazebo robot simulation software is used to simulate the field flight test, and the simulation flight test conditions are as follows:

Flight platform: quadcopter UAV×2

Ground platform: Ubuntu18.04 terminal

Test environment: multi-column obstacle map

Test platform: Processor: i5-10400F (six cores and twelve threads, CPU main frequency 2.9GHz), Graphics card: NVIDIA Geforce GTX 1660S (graphics memory 6GB)

Flight duration: 100s

The simulation flight test is demonstrated using an independent high-performance computer, which hosts the ROS+Gazebo joint simulation platform. Before the simulation flight test of the formation fault-tolerant control algorithm with distributed self-triggering strategy, three quadcopters were tested individually by turning on a simple ground station through the roslaunch command. Through the test, the computer can meet the simulation test with two quadrotor UAVs at the same time. After the computer performance test is passed, the formation fault-tolerant control algorithm with distributed self-triggering strategy is embedded into the control program to carry out the simulation flight test of the formation control algorithm.

2.3.2 Field flights

In this subsection, the deployment of the formation control algorithm with distributed self-triggering strategy for fault-tolerant control of formations on the DUSS hardware platform will be presented, and the algorithm parameter values obtained after simulation flight test tests will be considered to be applied to the field flight tests the field flight test conditions are as follows:

Flight platform: DJI M300 quadcopter UAV × 2

Ground station: three-screen laptop

Communication band: 1.4 GHz

Operating bandwidth: 20 MHz

Flight duration: 100s

The flight platform used for the field test is two DJI M300 quadcopters, which support the OSDK development mode and at the same time reduce the coupling of the DUSS modules. The quadcopter machines of the DJI M300 series are connected to the on-board calculation machine through the OSDK hardware expansion module, and the on-board computer and the OSDK expansion module use the serial port communication mode. A three-screen ruggedized laptop computer was used to host the ground station software for sending control commands for the UAV cluster, and the computer was also used to complete the communication test work before the flight test.

The final stage of the preparation for the field flight test is the deployment of the distributed self-triggering strategy fault-tolerant formation control algorithm on the onboard computer, using the OSDK open speed and position control interfaces to replace the conventional control program used in the Gazebo simulation, so as to make the onboard computer, the OSDK expansion module and the UAV flight control system hardware link between the link and the software compatibility. Once the above preparations are completed, the field flight test phase will begin.

3 Resultod

In this part, the proposed distributed self-triggered fault-tolerant control method is realized on a formation system which is made of two quadrotor unmanned aerial vehicles (UAVs). After that, simulation experiments and actual flight tests are conducted by us to verify the effectiveness and superiority of the method which is proposed in the present paper.

3.1 Dual UAV formation obstacle avoidance simulation test

In the course of obstacle avoiding for multiple unmanned aerial vehicle (UAV) formation tasks, a two-dimensional space is chosen to carry out simulation verification. The starting positions of two unmanned aerial vehicles are given by setting, which are $(-2,1)$, $(0.5,1.2)$, and setting the coordinate positions of obstacles $(-0.8,2.3)$, $(0.9,3.1)$, $(2.3,2.2)$, $(3.1,4.2)$, $(0.1,4.6)$, $(4.5,3)$, $(5.4,1.6)$, $(4.6,5.8)$. The range of the influence of barriers is determined as 0.5, and the safety distance between unmanned aerial vehicles (UAVs) is settled at 0.5. After that, the starting position of the building of two unmanned aerial vehicles in a two-dimensional space is shown in Figure 2.

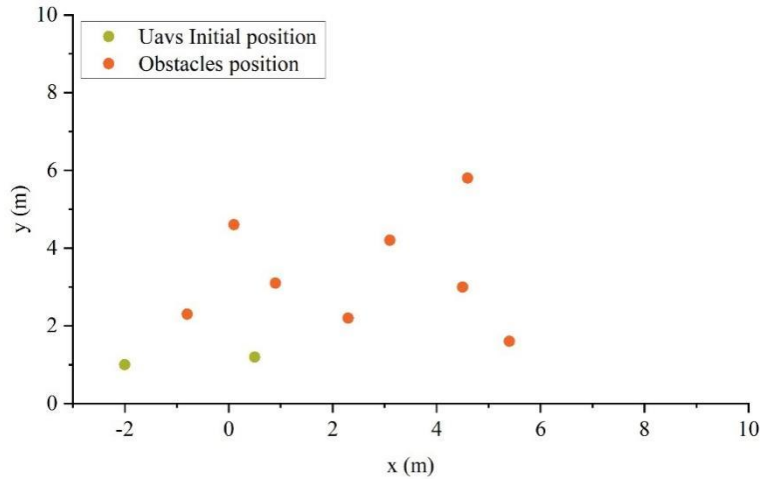


Figure 2: The initial position of a two-uavs in two dimensional space

Figure 3 shows the barrier evading process of the two unpiloted air vehicles (UAVs). To speak concretely, Picture (a) gives the UAVs' places after 1 second of working, and Picture (b) displays their positions after 2.5 seconds of working. From the figure we can see that, after the UAV swarm enters the region that has obstacles, the UAV formation cannot maintain the preset standard formation. On the contrary, every UAV plays the role of an independent individual and carries out obstacle avoidance work on its own. Moreover, in the course of the obstacle-avoiding procedure, there exists neither a collision between unmanned aerial vehicles (UAVs) nor the problem of falling into the trap of local minima. This therefore indicates that the algorithm which is put forward in this paper meets the standards for UAV formation obstacle avoidance.

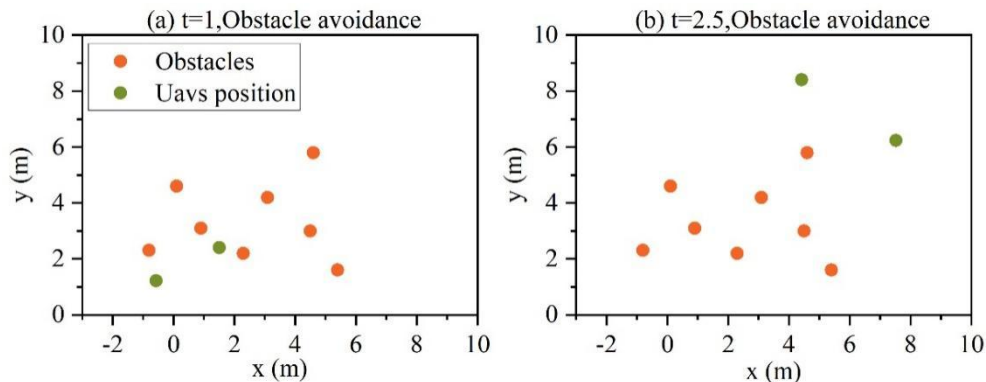


Figure 3: Uav's avoidance process

After the unmanned aerial vehicles (UAVs) leave the obstacle area, every UAV carries out self-re-configuration by itself. Figure 4 has drawn the whole forming route of these two unmanned aerial vehicles. The formation fault-tolerant control algorithm that depends on the distributed self-triggering strategy which this paper puts forward can reach the expected obstacle avoidance target for the dual UAV formation.

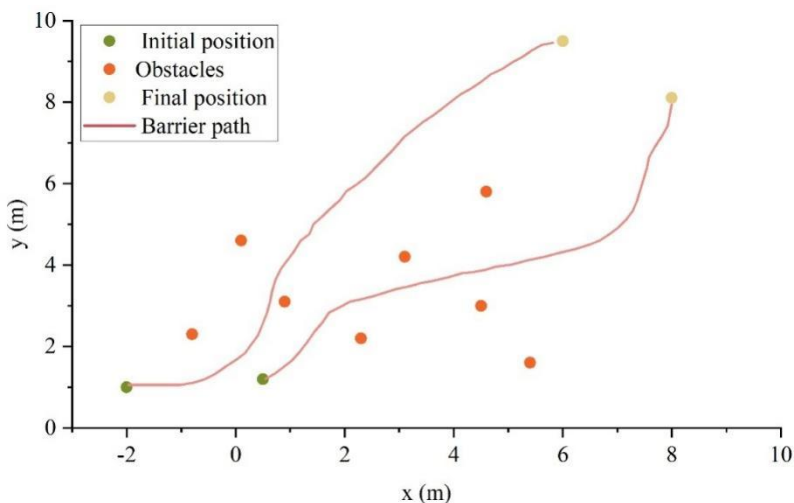


Figure 4: The overall formation of the two uavs

3.2 Field flight tests

3.2.1 Trajectory tracking response analysis

For the purpose of confirming the effect of the arithmetic method which this research has put forward, experiments are carried out upon this arithmetic method for the locus following of the position controlling system and the locus following response of the attitude controlling system. The tracking response test results of the position control system regarding the algorithm put forward in this paper, in the x, y, z directions, are shown in Figure 5. The formation fault-tolerant control algorithm, which is built on the distributed self-triggering strategy that the research institute has put forward, can effectively inhibit the influence of parameter uncertainties and external interferences on the track tracking performance of the quadcopter unmanned aerial vehicle (UAV). In the end, it obtains a stable and mistake-free path following outcome. Under the stable condition, the path following error which is in directions of x, y and z is smaller than 0.05 meters.

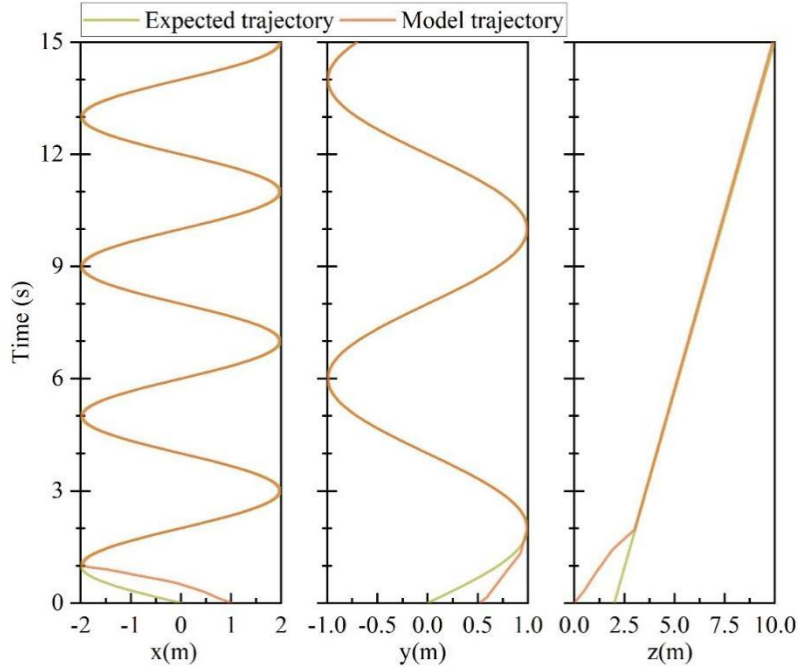


Figure 5: Position control system trajectory tracking response

Figure 6 gives the result results of the track following reaction for the posture control system which uses the algorithm that this paper puts forward. Concretely speaking, Figure (a) gives the simulation outcomes for the roll and pitch angles, meanwhile Figure (b) displays the simulation outcomes for the yaw angle. For the rolling angle and the pitching angle, there does not exist a fixed target moving path. It is obvious that, the algorithm which this paper has put forward can not only make the roll and pitch angles realize stability within 3 seconds, effectively decreasing the maximum overshoot value, but also brings about a small vibration range in the movement process of the unmanned aerial vehicle (UAV). With respect to the yaw angle, the algorithm is able to let it achieve convergence to the target trajectory in the scope of 2 seconds. The formation fault-tolerant control algorithm based on distributed self-triggering strategy in this paper has good tracking performance.

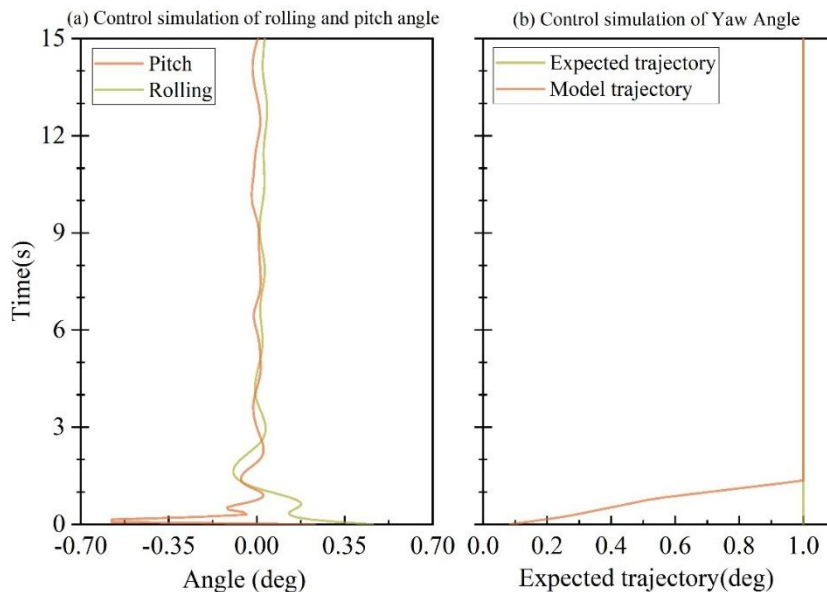


Figure 6: Attitude control system trajectory tracking response

3.2.2 Formation Hover 3D Trajectories

In this section the algorithm of this paper is subjected to a dual UAV cooperative formation hovering simulation experiment, this precondition assumes that unmanned aerial vehicles (UAVs) have the ability to share state-connected data and hence guarantees that there exists at least one directional connected graph inside the formation network. Figure 7 shows the three-dimensional flying track of a double-UAV group in the hovering process, therefore it describes the adjusting course which the group passes through in order to reach a hovering condition. In the whole process of the flight, the two unmanned aerial vehicles (UAVs) that are in formation continuously maintain the minimum distance which is needed for avoiding the occurrence of collisions. The structure still keeps complete, hence they finish the hovering task successfully. The control algorithm which this paper brings forward has the ability to rapidly and accurately track the expected motion path. Furthermore, it can satisfy the demands that formation flight control puts forward, both in the aspect of precision and the aspect of response speed.

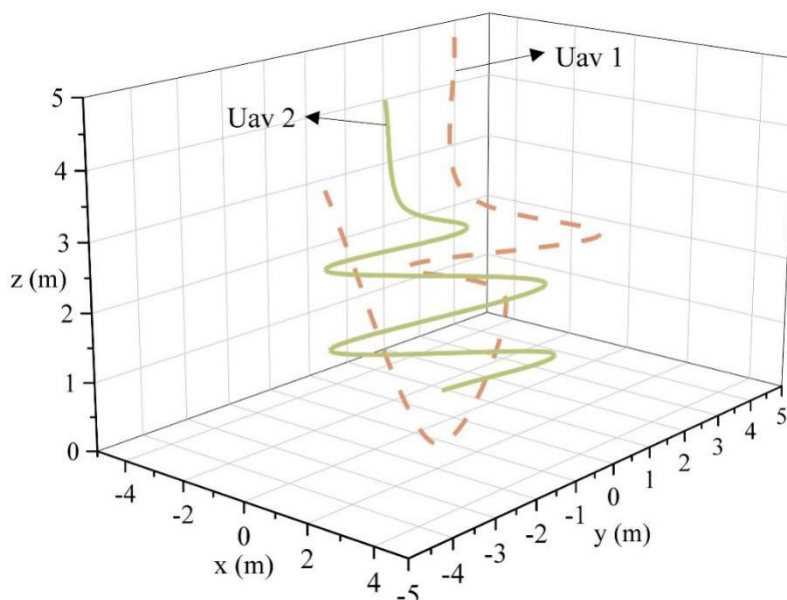


Figure 7: Three-dimensional formation trajectory

For the further explanation of the control accuracy of the algorithm which is put forward in this paper, Figure 8 shows the results of 3D time-varying formation trajectory tracking errors. In the first 10 seconds of the working process, the flying routes of the two unmanned aerial vehicles (UAVs) are in agreement with the pre-planned flight path. After the stable state is reached, the trajectory error is always kept within 0.03 meters, which therefore basically accords with the expected trajectory. The formation control algorithm that this paper puts forward, which is based on the distributed self-triggering strategy, can complete the dual UAV formation hovering task with high accuracy and has strong anti-interference abilities.

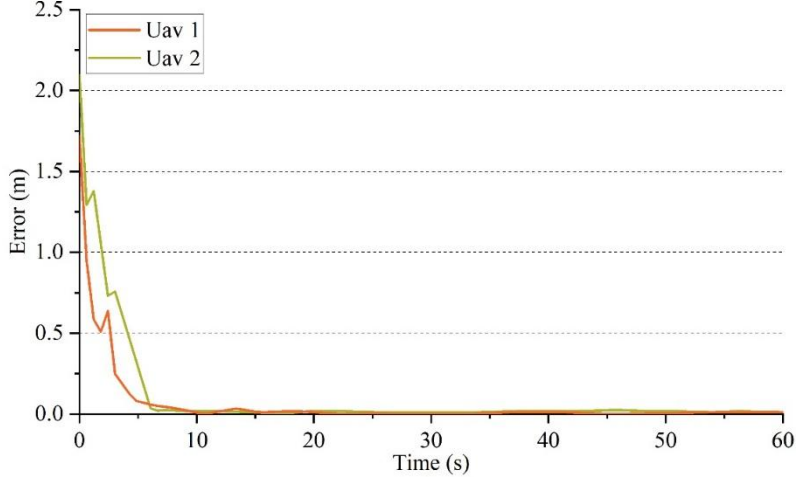


Figure 8: The three-dimensional time variable formation trajectory tracking error

3.2.3 Energy consumption measurements for formation flying

In this part, from the perspective of optimizing energy use, the effect of the formation fault-tolerant control algorithm which is built on the distributed self-triggering strategy is studied. This target is reached through making contrast on the energy consumption of the traditional algorithm with that of the algorithm which is put forward in the present paper. Furthermore, two groups of flight scene experiments along a straight-line path have been done by researchers. Two sets of two unmanned aerial vehicle formations are situated under different controlling mechanisms. One group is controlled by the traditional algorithm, therefore another is ruled by the algorithm which is put forward in this current paper. To the flight trajectory and the time parameters, they are same for both two groups of algorithms. The planned speed of the two unmanned aerial vehicle group when doing straight-line movement is set to 25 meters each second, and the destination course angle is 90 degrees.

Figure 9 gives the results of the energy consumption comparison that belongs to the dual UAV formation. To speak concretely, Figure (a) gives depiction of the energy consumption of UAV 1, and Figure (b) presents that of UAV 2. The energy difference which is shown by the shaded area in the figure is gotten through subtracting the energy consumption of the algorithm put forward in this paper from that of the traditional algorithm. The energy consumption of UAV 1 equipped with the traditional algorithm is around 7.1×10^5 J after stabilization, while the energy consumption of applying this paper's algorithm is only around 5.8×10^5 J. After it has reached the stable condition, the energy consumption of the two algorithms on Unmanned Aerial Vehicle (UAV) 2 is approximate 7.1×10^5 joules. The energy consumption rule of these two arithmetic methods on UAV 2 is on the whole coincident with that which is on UAV 1. Specifically speaking, the algorithm which is put forward in this current paper has lower energy consumption. Therefore, when we carry out the formation fault-tolerant control algorithm that this paper puts forward, which is established on a distributed self-triggering strategy, the dual UAV formation has a certain energy-saving effect.

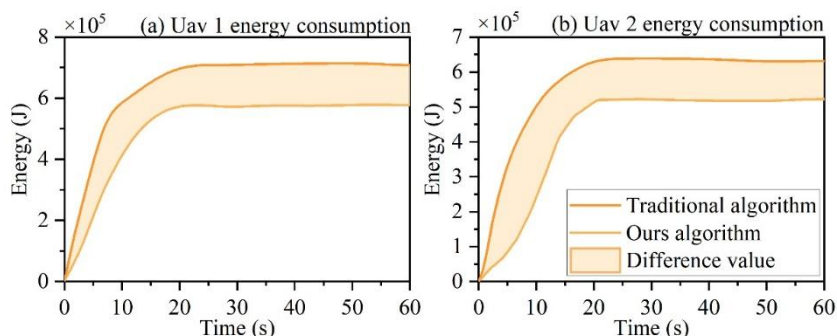


Figure 9: Comparison results of two-uavs energy consumption

4 Conclusion

In order to better design the dual UAV cooperative formation flight control algorithm, this article establishes a mathematics model for the unmanned aerial vehicle (UAV) system, and therefore puts forward a formation flight control algorithm which is built on a distributed self-triggering method, which realizes the acquisition of state information and error analysis of dual UAVs in formation flight. For the deeper research on the effect of this algorithm, simulation test works are conducted by us to check the influence of the algorithm on formation flight control. The result discoveries of this study are as what follows:

(1) The dual UAV equipped with the algorithm of this paper can effectively avoid all the obstacles and quickly reformat.

(2) In the field flight, the dual UAV formation system can be stabilized to the desired trajectory within 3s, and the error in all directions is small within 0.05m.

(3) Through making use of the algorithm which is put forward in this research work, the double unmanned aerial vehicle (UAV) formation system has the ability to rapidly and accurately complete the formation hovering task. Furthermore, the deviation which lies between its movement route and the designed moving track is smaller than 0.03 meters.

(4) The energy consumption of Unmanned Aerial Vehicle (UAV) groups which use the traditional algorithm is higher than 6×10^5 joules. By comparison, the energy use of UAV groups which carry out the algorithm put forward in this paper has got obvious reduction.

Funding

This work was supported by the Linxia Power Supply Company, State Grid Corporation of China, under grant B727142400XL.

About the Author

Hu Yarong, who is a woman person, possesses a bachelor academic degree. At current stage, she holds the position of associate senior engineer in State Grid Linxia Electric Power Supply Company. Her research interest regions include the running and maintenance of electric power systems, the controlling of grid security, and the dependability of distribution networks.

Ren Buyong is a man person, he has a bachelor degree. He is now holding a work position within the State Grid Linxia Power Supply Company, where he serves as an associate senior engineer. His current research focuses on emergency repair strategies, fault diagnosis in distribution networks, and improving power supply continuity.

Chen Sifan, who is a male person, possesses a master's academic degree. At current stage, he holds the post of engineer in State Grid Linxia Electric Power Supply Company. His research interest fields include the rebuilding of power grids after natural disasters, smart distribution systems, and the scheme design of power systems.

Junyun Shen, male, bachelor's degree. In current time, he holds the post of engineer at State Grid's Linxia Power Supply Company. His work focuses on customer-side energy management, customized electricity solutions for enterprises, and optimization of business environments in the power sector.

Yonglong Ma, male, master's degree. In current time, he holds the position of a high-rank engineer at the Linxia Power Supply Company which belongs to the State Grid. His professional interests lie in staff training and performance evaluation, technical capability development, and human resource management within electric utility companies.

References

- [1] Dong, X., Hua, Y., Zhou, Y., Ren, Z., & Zhong, Y. (2018). Theory and experiment on formation-containment control of multiple multirotor unmanned aerial vehicle systems. *IEEE Transactions on Automation Science and Engineering*, 16(1), 229-240.
- [2] Jiang, Y., Bai, T., & Wang, Y. (2022). Formation control algorithm of multi-UAVs based on alliance. *Drones*, 6(12), 431.
- [3] Shizhuang, W., Xingqun, Z. H. A. N., Yawei, Z. H. A. I., Cheng, C. H. I., & Jiawen, S. H. E. N. (2021). Highly reliable relative navigation for multi-UAV formation flight in urban environments. *Chinese Journal of Aeronautics*, 34(7), 257-270.
- [4] de Angelis, E. L., Giulietti, F., & Rossetti, G. (2018). Multirotor aircraft formation flight control with collision avoidance capability. *Aerospace Science and Technology*, 77, 733-741.
- [5] Hu, J., Wang, L., Hu, T., Guo, C., & Wang, Y. (2022). Autonomous maneuver decision making of dual-UAV cooperative air combat based on deep reinforcement learning. *Electronics*, 11(3), 467.
- [6] Jiang, S., Xie, W., Zhang, L., Zhang, G., Liang, X., & Zheng, Y. (2024, November). Current status and development trends of research on autonomous decision-making methods for unmanned swarms. In *International Conference on Optics, Electronics, and Communication Engineering (OECE 2024)* (Vol. 13395, pp. 132-138). SPIE.
- [7] Lutz, R. R., Frederick, P. S., Walsh, P. M., Wasson, K. S., & Fenlason, N. L. (2017). Integration of unmanned aircraft systems into complex airspace environments. *Johns Hopkins Apl Technical Digest*, 33(4), 291-302.
- [8] Liang, Z., Li, Q., & Fu, G. (2023). Multi-UAV collaborative search and attack mission decision-making in unknown environments. *Sensors*, 23(17), 7398.
- [9] Ghamry, K. A., Dong, Y., Kamel, M. A., & Zhang, Y. (2016, June). Real-time autonomous take-off, tracking and landing of UAV on a moving UGV platform. In *2016 24th Mediterranean conference on control and automation (MED)* (pp. 1236-1241). IEEE.

- [10] Li, J., Liu, J., Huangfu, S., Cao, G., & Yu, D. (2023). Leader-follower formation of light-weight UAVs with novel active disturbance rejection control. *Applied Mathematical Modelling*, 117, 577-591.
- [11] Pan, C., Zhou, L., Xiong, P., & Xiao, X. (2018, July). Robust adaptive dynamic surface tracking control of an underactuated surface vessel with unknown dynamics. In 2018 37th Chinese Control Conference (CCC) (pp. 592-597). IEEE.
- [12] Liu, H., Meng, Q., Peng, F., & Lewis, F. L. (2020). Heterogeneous formation control of multiple UAVs with limited-input leader via reinforcement learning. *Neurocomputing*, 412, 63-71.
- [13] Nägeli, T., Conte, C., Domahidi, A., Morari, M., & Hilliges, O. (2014, September). Environment-independent formation flight for micro aerial vehicles. In 2014 IEEE/RSJ International Conference on Intelligent Robots and Systems (pp. 1141-1146). IEEE.
- [14] Fareh, R., Baziyad, M., Rabie, T. F., Khadraoui, S., & Rahman, M. H. (2024). Efficient Path Planning and Formation Control in Multi-Robot Systems: A Neural Fields and Auto-Switching Mechanism Approach. *IEEE Access*.
- [15] Cheng, W., Jiang, B., Zhang, K., & Ding, S. X. (2021). Robust finite-time cooperative formation control of UGV-UAV with model uncertainties and actuator faults. *Journal of the Franklin Institute*, 358(17), 8811-8837.
- [16] Zhang, Z., & Duan, H. (2024). Distributed velocity-free formation tracking control for clustered UAVs under virtual leader-follower framework. *Science China Technological Sciences*, 67(5), 1538-1552.
- [17] Zhang, J., Yan, J., & Zhang, P. (2020). Multi-UAV formation control based on a novel back-stepping approach. *IEEE Transactions on Vehicular Technology*, 69(3), 2437-2448.
- [18] Dang, L., & Shen, Z. (2022, August). Coordinated control of load transportation system for multiple quadrotor UAVs. In 2022 34th Chinese Control and Decision Conference (CCDC) (pp. 4683-4687). IEEE.
- [19] Luis, C. E., Vukosavljev, M., & Schoellig, A. P. (2020). Online trajectory generation with distributed model predictive control for multi-robot motion planning. *IEEE Robotics and Automation Letters*, 5(2), 604-611.
- [20] Bolandi, H., Moradi Pari, H., & Izadi, M. R. (2022). Multiple spacecraft formation and station-keeping control in presence of static attitude constraint via decentralized virtual structure approach. *Journal of Aerospace Engineering*, 35(1), 04021104.
- [21] Fang, J., Han, Y., Zhou, Z., Chen, S., & Sheng, S. (2021, August). The collaborative combat of heterogeneous multi-UAVs based on MARL. In *Journal of Physics: Conference Series* (Vol. 1995, No. 1, p. 012023). IOP Publishing.
- [22] Vásárhelyi, G., Virágh, C., Somorjai, G., Nepusz, T., Eiben, A. E., & Vicsek, T. (2018). Optimized flocking of autonomous drones in confined environments. *Science Robotics*, 3(20), eaat3536.

- [23] Costa, A. N., Medeiros, F. L., Dantas, J. P., Geraldo, D., & Soma, N. Y. (2022). Formation control method based on artificial potential fields for aircraft flight simulation. *Simulation*, 98(7), 575-595.
- [24] Seo, J., Kim, Y., Kim, S., & Tsourdos, A. (2012). Consensus-based reconfigurable controller design for unmanned aerial vehicle formation flight. *Proceedings of the Institution of Mechanical Engineers, Part G: Journal of Aerospace Engineering*, 226(7), 817-829.
- [25] Moreira, M. S. M., Villa, D. K. D., & Sarcinelli-Filho, M. (2024). Controlling a virtual structure involving a uav and a ugv for warehouse inventory. *Journal of Intelligent & Robotic Systems*, 110(3), 121.
- [26] Dai, S. L., He, S., Lin, H., & Wang, C. (2017). Platoon formation control with prescribed performance guarantees for USVs. *IEEE Transactions on Industrial Electronics*, 65(5), 4237-4246.
- [27] Wang, N., & Xu, H. (2020). Dynamics-constrained global-local hybrid path planning of an autonomous surface vehicle. *IEEE transactions on vehicular technology*, 69(7), 6928-6942.
- [28] Zhou, X., Wu, P., Zhang, H., Guo, W., & Liu, Y. (2019). Learn to navigate: cooperative path planning for unmanned surface vehicles using deep reinforcement learning. *Ieee Access*, 7, 165262-165278.
- [29] Chung, T. H., Clement, M. R., Day, M. A., Jones, K. D., Davis, D., & Jones, M. (2016, May). Live-fly, large-scale field experimentation for large numbers of fixed-wing UAVs. In *2016 IEEE International Conference on Robotics and Automation (ICRA)* (pp. 1255-1262). IEEE.
- [30] Brandao, A. S., Barbosa, J. P., Mendoza, V., Sarcinelli-Filho, M., & Carelli, R. (2014, May). A multi-layer control scheme for a centralized uav formation. In *2014 International Conference on Unmanned Aircraft Systems (ICUAS)* (pp. 1181-1187). IEEE.